INTERNATIONAL ATOMIC ENERGY AGENCY
UNITED NATIONS EDUCATIONAL, SCIENTIFIC AND CULTURAL ORGANIZATION
INTERNATIONAL CENTRE FOR THEORETICAL PHYSICS
I.C.T.P, P.O. BOX 586, 34100 TRIESTE, ITALY, CABLE: CENTRATOM TRIESTE

H4-SMR 1012 - 35

AUTUMN COLLEGE ON PLASMA PHYSICS

13 October - 7 November 1997

The Electron Beam Plasma Instability: Space Observations, Theory and Simulation

C.T. DUM

Max-Planck Institut für Extraterrestrische Physik,
Garching, Germany

These are lecture notes, intended for distribution to participants.

THE ELECTRON BEAM PLASMA INSTABILITY: SPACE OBSERVATIONS, THEORY AND SIMULATION

C. T. Dum*
Max Planck Institut für Extraterrestrische Physik, D85740 Garching, Germany

I. INTRODUCTION

Electron beams have many applications and occur frequently in space plasmas. The beam can provide a free energy source for various instabilities. In a weakly magnetized plasma, such as is found in interplanetary space, a gentle beam excites the well known Langmuir waves with frequencies close to the electron plasma frequency. Observations in the Earth's and other planetary electron foreshock regions have shown, however, that frequencies substantially above and below the plasma freuency can also be excited by then electron beam which is formed by electrons reflected from the bow shock. We explain these upshifted and downshifted oscillations in terms of an instability of a relatively cold and intense beam. In a magnetized plasma, such as occurs in the auraral zones, electron beams can drive a whole variety of instabilities. In addition to Langmuir waves which propagate in the direction of the beam, the highly obliquely propagating upper and lower hybrid waves are of particular interest. The lower hybrid modes (Auroral Hiss) can transversely heat ions through ion cyclotron resonances. Combined with the magnetic mirror force upward moving ion conics (named for their conic shaped velocity distribution function)can thus be generated. Such conics of ionospheric origins are observed along auroral magnetic field lines at great distances from the Earth.

We will use linear theory, including numerical solutions of the dispersion relation, to study the instability mechanisms. Computer simulation studies will be used to analyze various nonlinear aspects. A particular advantage of simulation is that one can separate various effects by e.g. first using a hybrid model with only the beam represented by particles while the bulk plasma is represented by fluids. In the next step, the bulk electrons are also represented by particles. And finally, by also representing the ions as particles, one finds that they are responsible for a number of important nonlinear effects, such as the scattering of plasma waves into backscattered waves and into a (modified) Langmuir condensate. Similarly, in case of a plasma in a magnetic field, one may compare wave excitation for unmagnetized ions, an approximation often used in theoretical studies of lower hybrid waves, with the case of complete ion dynamics.

---

*Also at the Center for Space Research, Massachusetts Institute of Technology, Cambridge, MA 02139.

II. LINEAR DISPERSION RELATION FOR ELECTRON PLASMA WAVES

The basic oscillations of a plasma without a magnetic field are Langmuir waves, with frequencies close to the electron plasma frequency, and ion sound waves with freqencies typically below the ion plasma frequency. One can find these modes from a fluid model. In the case of Langmuir waves, both electrons and ions are adiabatic, whereas for ion sound the electrons are isothermal. Kinetic theory reveals, however, that ion sound waves are heavily damped, unless the ions are much colder than the electrons. Kinetic theory also shows that ion sound waves are most easily excited by a relative electron - ion drift, a current, whereas Langmuir waves are excited by a beam, corresponding to a bump (positive slope) in the far tail of the electron distribution. In contrast to these **kinetic** instabilities, a corresponding fluid model gives rise to **reactive** wave modes, which either are complex conjugate (unstable - damped) solutions of the dispersion relation, or are undamped (real solution).

Kinetic theory, as the more complete description, contains the hydrodynamic models as limiting cases. In case of very large relative electron -ion drifts one obtains the well known reactive **Buneman two stream instability**. What apparently is not recognized sufficiently, however, is that the usual textbook approximations for the kinetic instability of Langmuir waves require a extremely tenous and very broad beam, a condition which mostly is not met in laboratory or simulation studies, but as the elecron foreshock observations imply, also not always in nature.

The usual textbook approximation says that the growth rate is determined by the slope of the distribution function at the phase velocity which in turn determines the imaginary part of the dielectric constant and Landau damping/growth. The real frequency is assumed to be given by the well known dispersion relation for Langmuir waves, in the absence of a beam. It turns out however, that the beam can strongly affect even the topology of the dispersion relation. This toplogy is determined by a coupling between fast and slow beam modes with phase velocities slightly larger and smaller than the beam speed, and corresponding fast and slow branches of the plasma wave mode $\omega \approx \omega_e$. The topology is modified as the beam spread increases. At a critical, but surprisingly large beam spread, e.g.$v_b/u \approx 0.35 for n_b/n = 0.01$, the fast and slow plasma branch reconnnect by disconnecting from the beam modes. This signals the transition from reactive to kinetic instability. However, a "bump" in the dispersion relation at the phase velocity corresponding to the beam spead remains and significantly affects nonlinear processes (which depend on frequency differences) at even much larger beam spreads or smaller beam densities. This will be shown in simulation studies of Langmuir waves and by a corresponding extended turbulence theory.

If the beam does not meet the criteria for kinetic instability, but is intense and/or cold, than the beam modes can be excited, with frequencies substatially below or above the plasma frequency. The latter occurs for very narrow beams with small drifts (in the range of the electron thermal velocity). The mechanism for these downshifted oscillations is most easily understood in terms of the more familiar excitation of ion acoustic waves, with the electron beam assuming the role of the ions. Hence the requirement of a vary narrow beam, in order to avoid Landau damping by the beam is also easily understood. Frequencies substantially above the plasma frequency can be excited by a very cold beam with drift velocities in the range of $u \approx 5v_e$. The mode (slow beam mode) is a negative energy wave which is destabilized through Landau damping by bulk electrons. Finally, if both the thermal velocities of the beam and bulk electrons are negligible compared to the drift velocity, a purely reactive instability with a sharp cutoff near the plasma frequency is excited by a phase bunching mechanism. The conditions for this fluid type instability are, however, much more stringent than is generally stated [*Dum*, 1989].

III. SIMULATION STUDIES OF BEAM-PLASMA INSTABILITY IN THE UNMAGNETIZED PLASMA

Linear instability theory is an essential design tool for simulation studies. Applied to our case, this theory provides the design parameters for the study of Langmuir wave instability, reactive instability and downshifted oscillations. In addition to appropriate beam and plasma parameters, it is crucial for a comparsion with statistical turbulence theories, to always allow many unstable wave modes by choosing a sufficiently large system.(For periodic boundary conditions, wave numbers are discretized by the system length, $k = 2\pi m/L$. Both conditions were not met in the early simulations attempting to verify quasilinear theory of stabilization by plateau formation. Particle trapping was instead found to be the stabilization mechanism. With the weak beams required for kinetic instability, a large number of simulation particles is required to overcome the thermal noise level, a condition which was also difficult to meet in the early simulations. Now, however, with an appropriately designed simulation one can verify quasilinear theory [*Dum*, 1990a).

One can also show the transition from reactive to kinetic instability as an initially very narrow beam widens due to diffusion [*Dum*, 1990b], as well as the kinetic effects in the generation of downshifted oscillations [*Dum*, 1990c]. A particularly useful tool in these studies is a numerical code for the solution of the dispersion relation with the actual evolving and strongly non-Maxwellian distribution functions, as demanded by quasilinear theory. The evolution of the distribution functions not only modifies the growth rate, but also leads to changes of the real wave frequencies, and even a change in

the topology of the dispersion relation and the nature of the instability.

Even quasilinear theory can be verified to a high degree of accuracy, there are interesting (long term) nonlinear effects, such as scattering to backward propagating waves, formation of a Langmuir condensate at very small wave numbers and then formation of a secondary condensate at the phase velocity corresponding to the beam [*Dum*, 1990a, *Muschietti and Dum*, 1991]. By comparing models without ions, with an ion fluid and with fully kinetic ions, it is established that scattering off ions (nonlinear Landau damping) ist mostly responsible for these nonlinear processes.

While for the fundamental studies of instabilities a periodic homogeneous system is most appropriate, it appears very desirable to account for the injection mechanism of beam particles, in particular. Without continous injection of fresh beam particles it is difficult to explain how an instability can be maintained in view of effective quasilinear stabilization, although various nonlinear processes have been invoked. From detailed studies of solar flare related beam propagation and related excitation of Langmuir waves and radio bursts, the important role of convection (time of flight) effects in regenerating a beam is understood. Another consistent, but very puzzling observational feature is the burstyness of Langmuir waves. Although single spacecraft cannot distinguish temporal variations from spatial features being passed, the interpretation is usually in terms of spatially localized wave bursts. Explanations range from strong turbulence effects, stochastic wave growth affected by ambient density fluctuations to electron beam nonlinearities [*Muschietti et al.*,, 1996].

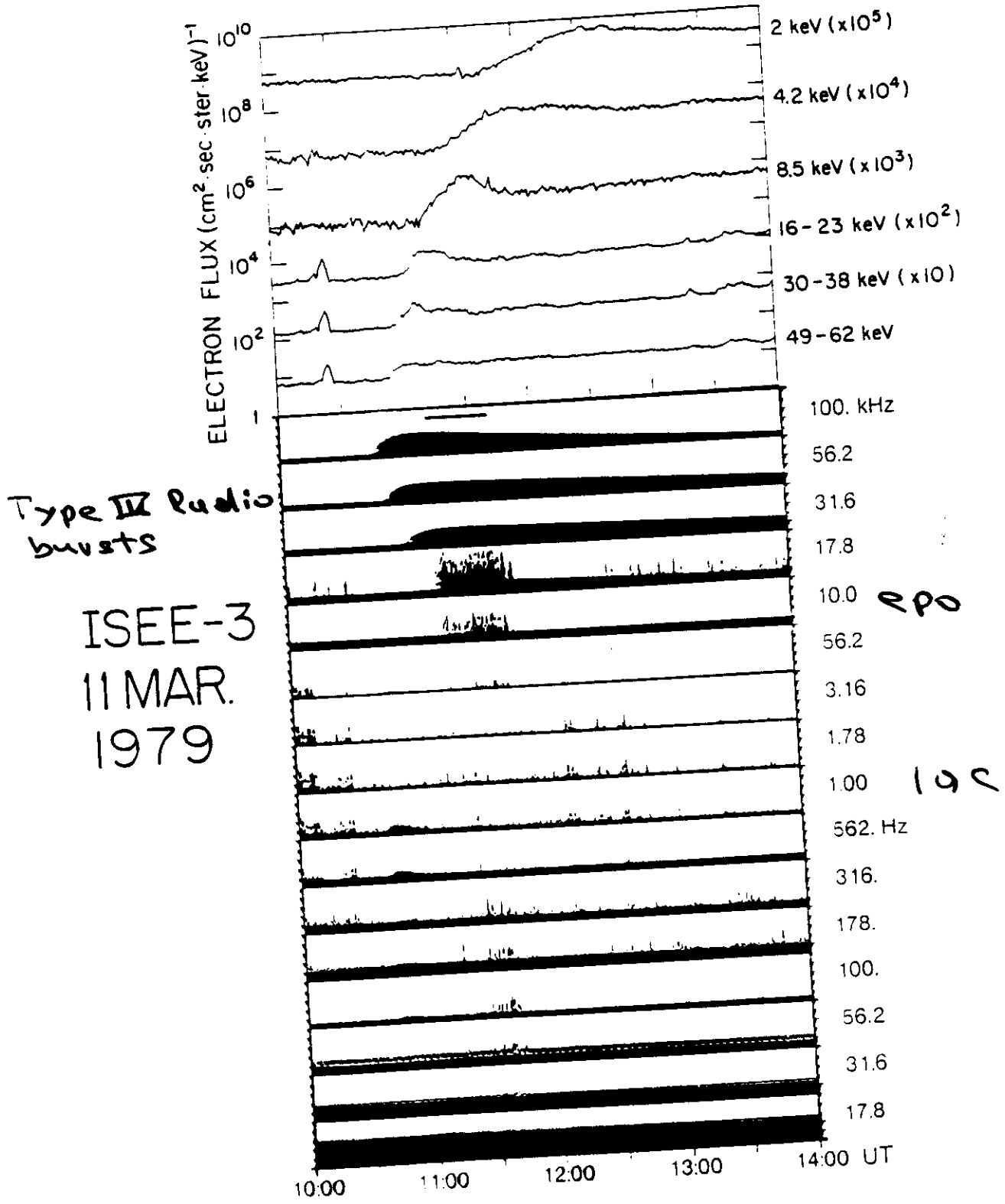
ELECTRON FLUX (cm² · sec · ster · keV)⁻¹
10¹⁰
10⁸
10⁶
10⁴
10²
1
2 keV (x10⁵)
4.2 keV (x10⁴)
8.5 keV (x10³)
16-23 keV (x10²)
30-38 keV (x10)
49-62 keV
100. kHz
56.2
31.6
17.8
10.0
56.2
3.16
1.78
1.00
562. Hz
316.
178.
100.
56.2
31.6
17.8
10:00
11:00
12:00
13:00
14:00 UT
Type III Radio bursts
ISEE-3
11 MAR.
1979
epo
19c

Fig. 1

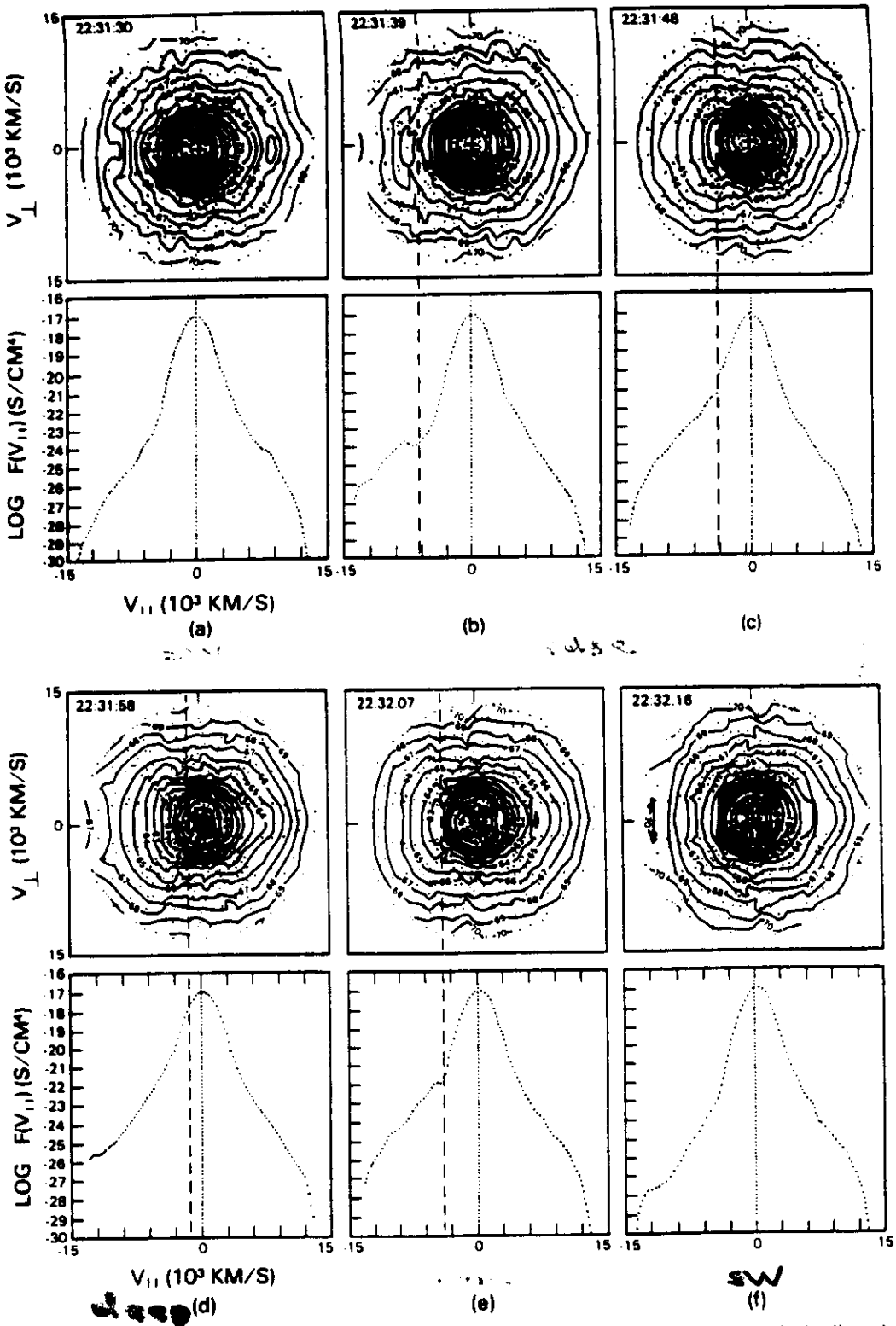

Fig. 1. An example of an ISEE 1 crossing from (*a*) the solar wind into (*b* and *c*) the region at the leading edge of the electron foreshock, and to (*d*) a point deep in the foreshock. Between Figures 1*d* and 1*e* the relative motion reverses, and ISEE 1 (*e*) again crosses the leading edge of the foreshock and (*f*) returns to the solar wind. The contour plots are a sequence of measurements of $f(v_\parallel, v_\perp)$ made by the ISEE 1/GSFC vector electron spectrometer on November 7, 1977, between 2231:30 and 2232:16 UT. Contours of $-\ln_e f$ are plotted on a $v_\perp$ (vertical) and $v_\parallel$ (horizontal) grid. The contour spacing is unity in $\ln_e$ space; the innermost contour is $-\ln_e f = 57$. Below each contour plot are the reduced distributions $F(v_\parallel)$ calculated from $f(v_\parallel, v_\perp)$.

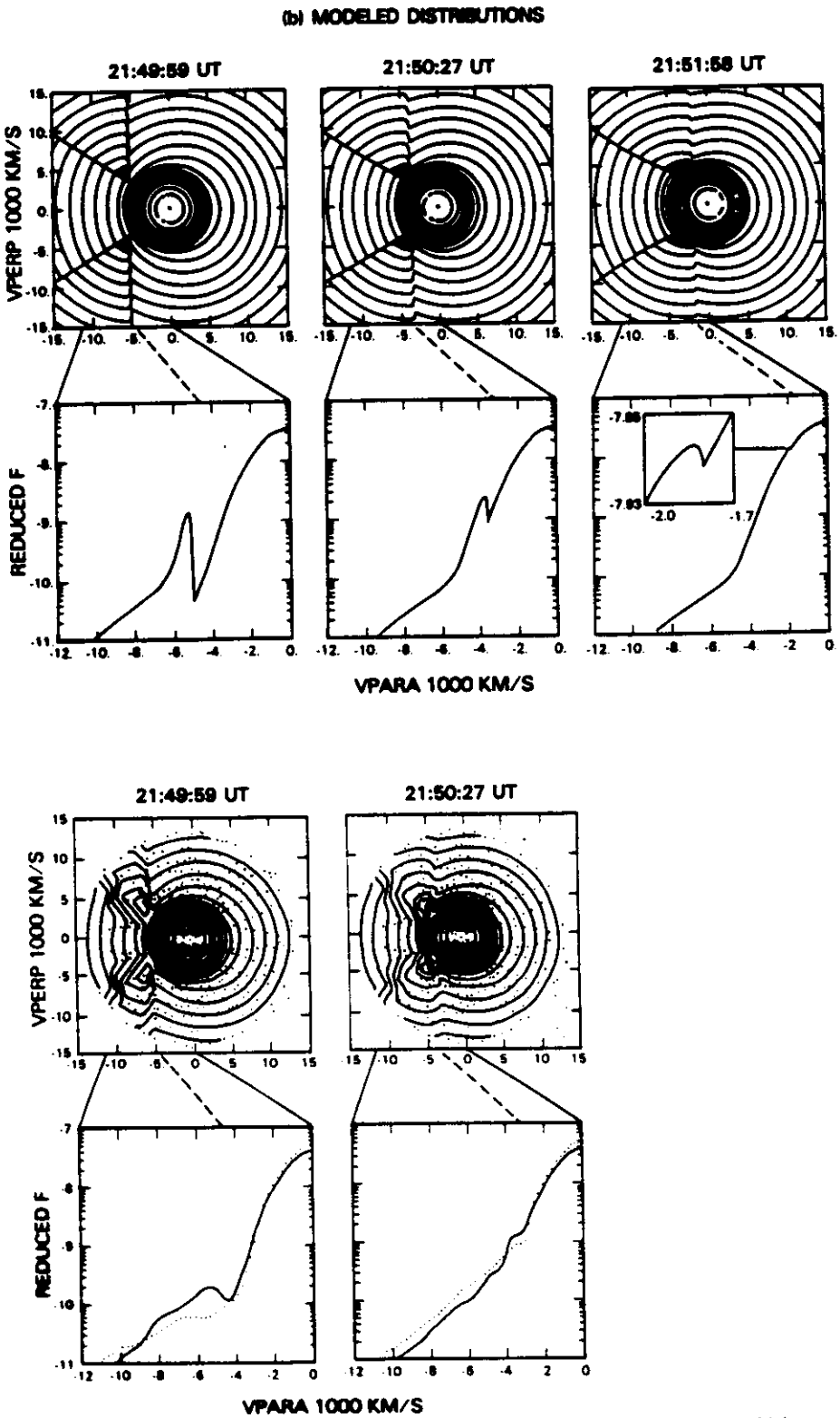

Model

Model.
incl. instrument function.

dots (dotted)

Fig. 7*b*. Modeled distributions (upper three panels) at locations in foreshock coordinates which are the same as those for the observations shown in Figure 7*a*. See Table 2 and the text for discussion. The modeled two-dimensional distributions in the top panels corresponding to the observations at 2149:59 UT and 2150:27 UT have been decimated to simulate the instrument sampling and are shown below in the lower panels. Reduced distributions have been computed from them and plotted in the two bottom panels (solid curves) along with the observed reduced distributions, replotted on this expanded velocity scale and shown as dotted curves. The similarity and contrast between model and data are discussed in the text.

Energization Mechanism

T C. S. WU JGR 84
M. M. Leroy, A. Mangeney Ann. Geophys. 1984

O Feldmun et al, JGR 83

Fermi process : moving magnetic mirror

(+ acc. potential)

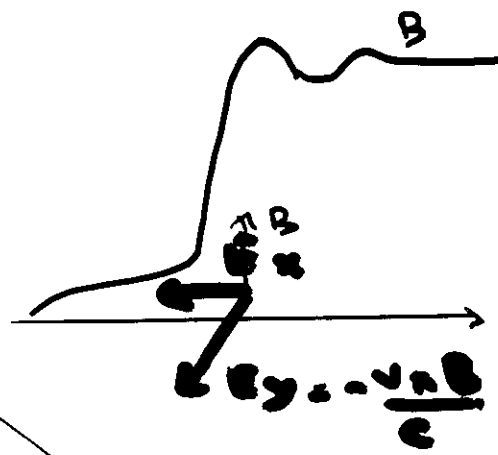

Electron motion:

$$E = \frac{m v_{\parallel}^2}{2} + \mu B - |e| \phi = \text{const}$$

$$\mu = \frac{m v_{\perp}^2}{2B} = \text{const}$$

in de Hoffmun – Teller frame

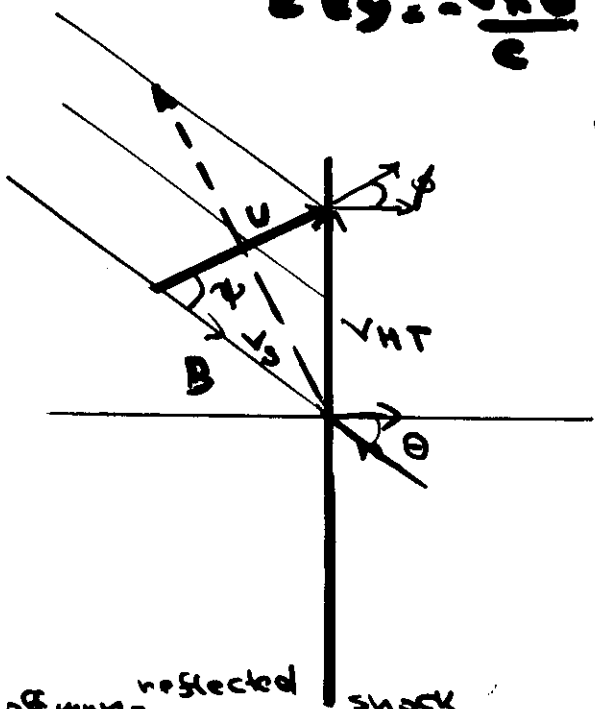

de Hoffmun-Teller frame:

upstream (solar wind) flow $\parallel B$ by drift along shock surface

$$\underline{v}_s = \underline{u} - \underline{v}_{HT} \parallel B$$

$$\underline{v}_{HT} = \frac{\underline{n} \times (\underline{u} \times \underline{B})}{\underline{n} \cdot \underline{B}}$$

$$\underline{v}_s = \frac{\underline{u} \times \underline{n} \cdot \underline{B} - \underline{n} \cdot \underline{B}\, \underline{u} + \underline{n} \cdot \underline{u}\, \underline{B}}{\underline{n} \cdot \underline{B}}$$

$$v_s = \frac{\cos\phi}{\cos\theta} u \, \hat{\underline{v}}$$

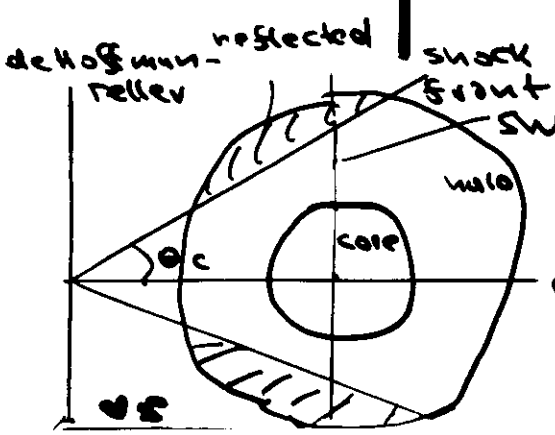

elastic refl.: $\underline{v}_s \to -\underline{v}_s$

$$\underline{v}_2 = -\underline{v}_s + \underline{v}_{HT} = -\underline{v}_1 + 2\underline{v}_{HT}$$

$\sin^2 \theta_c = \frac{B_1}{B_2}$

Electron Fore shock

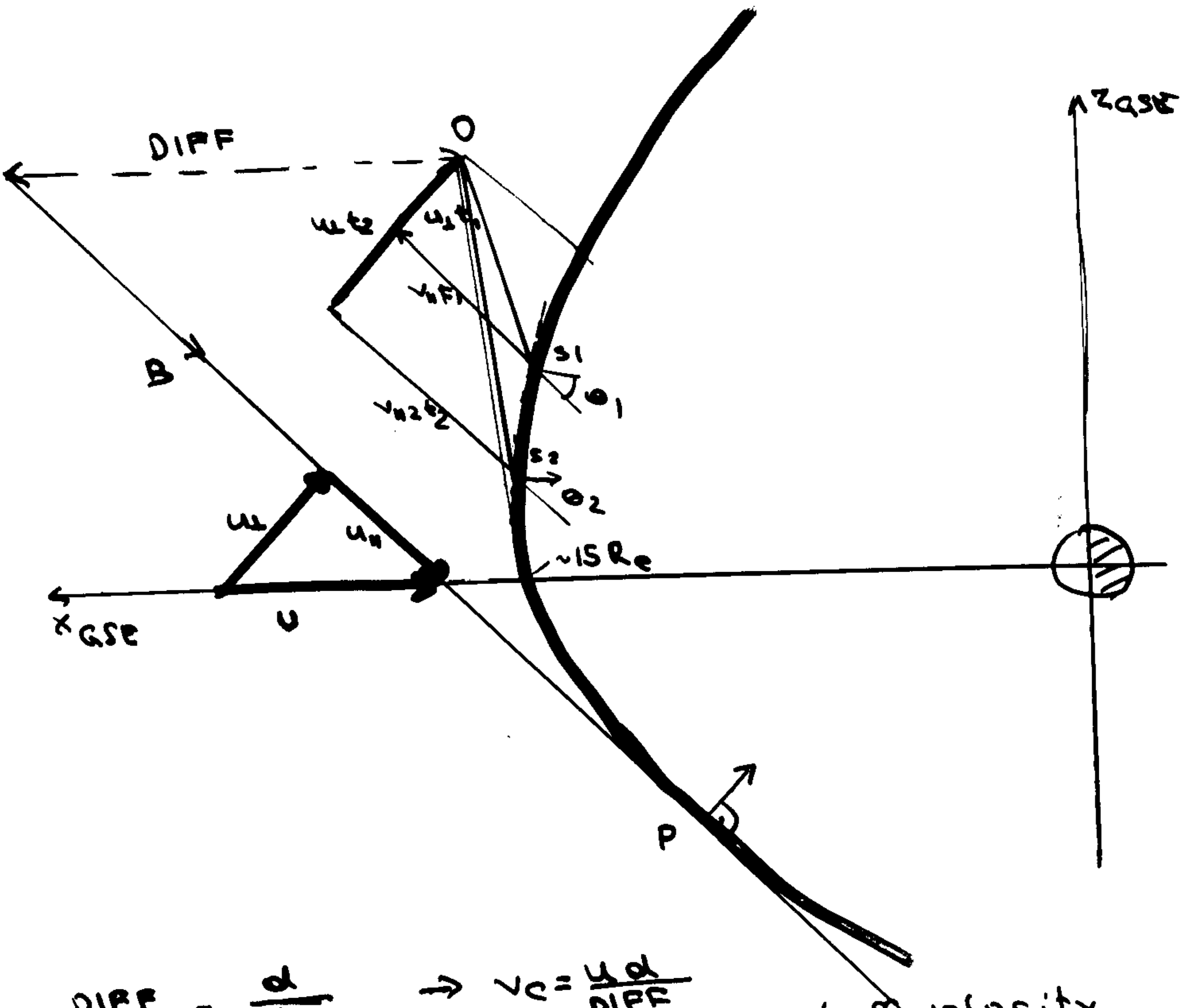

$$t = \frac{DIFF}{u} = \frac{d}{v_c} \rightarrow v_c = \frac{u\,d}{DIFF}$$ cutoff velocity

Filbert & Kellog JGR 1979

CAIRNS 1987

FITZENREITER SCUDDER KLIMAS 1990

ONSAGER & HOLZWORTH 1990 (CAMPS)

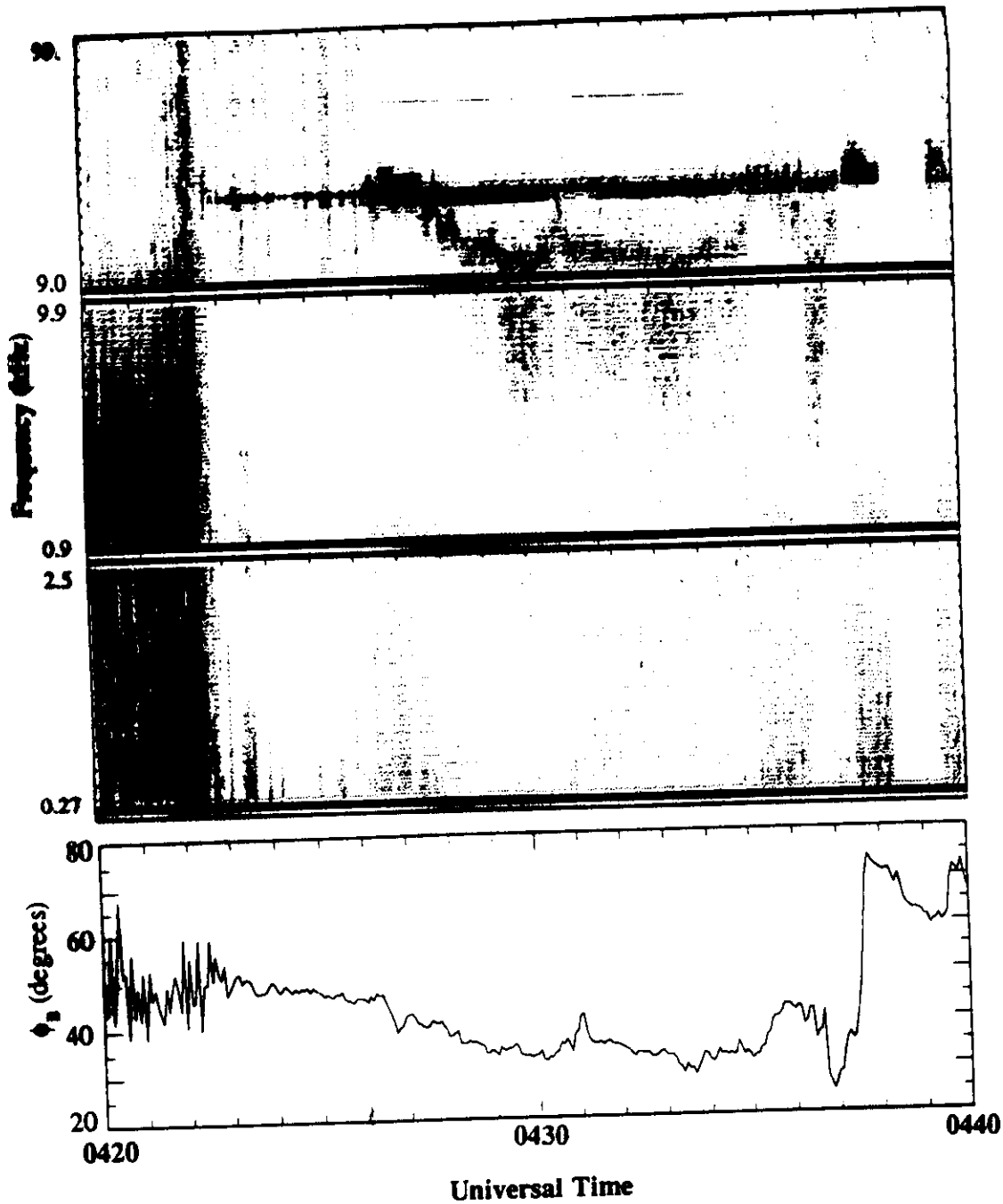

Fig. 1. The electric field intensity (upper three panels) and magnetic field direction (lower panel) during a transition from the magnetosheath to the solar wind. Langmuir waves are detected upstream from the shock at about 39 kHz. Beginning near 0426:30 UT, the electron beam mode is seen as a band distinct from the Langmuir waves, first increasing above f_{pe}, then decreasing below f_{pe}. The electron beam mode frequency is correlated with the direction of the magnetic field.

Wave observations

Fredricks et al. 1968 — $\omega \approx \omega_{pe}$

Scarf et al 1971 — 600-300 eV electrons

Gurnett & Anderson 1977
Gurnett & Frank 1978 — doppler sh. ion acoustic waves

Anderson et al 1981 — corr. with e & ion beams

Filbert & Kellog 1979 — ω_{pe}, cutoff mech., instability, beam prop.

Foreshock

Etcheto, Faucheux 1984

$\omega \approx \omega_{pe}$

$\omega \gtrless \omega_e$

$\frac{W}{nT_e}$

Lacombe, Mangeney, Harvey, Scudder 1985

bursts (15 - 30 msec)

beam model

Cairns 1989
1990

$\hat{T}_b = \left(\frac{V_b}{u}\right)^2 \propto \hat{n}_b = \frac{n_b}{n}$

Moses et. al (Jupiter, $n_b \gg$)
1984

Fuselier, Gurnett, Fitzenreiter 1985

Downshifted oscillations

$\omega < \omega_e$

AMPTE — Onsager Holzworth, 1990
Koons et al. 1987

Recent observations: WIND spacecraft, cf. Fitzenreiter et al GRL 1996

The Electron Beam Instability and Turbulence Theories

C. T. Dum

Max-Planck-Institut für Physik u. Astrophysik, Institut für extraterrestrische Physik

D-8046 Garching, Federal Republic of Germany

1. Introduction: Observations
2. Linear Instability Theory
   (a) Fluid Model, Kinetic Theory
   (b) Transition from Reactive to Kinetic Instability
3. Dynamics of the Wave-Beam Interaction and Quasi-linear Theory: Hybrid Simulations efl–b
4. Interaction with the Bulk Plasma and Mode Coupling
   Simulation Models:
   (a) e–b: Plateau formation
   (b) e–ifl–b: Resonant Mode Coupling to Ion Sound
   (c) e–i–b: Nonlinear Landau Damping
   (d) Strong Turbulence Theory

1. Introduction: Observations

Observed Electron Beams

	$\hat{n}_b = n_b/n_e$	u/v_e	v_b/u
Foreshock (Earth)	$10^{-3} - 0.05$	1 – 10	$0.2 - 0.3$
Type III bursts	10^{-5}	20	$0.1 - 0.2$
Aurora(magnetized)	$10^{-6} - 10^{-3}$	30 – 100	$0.1 - 0.5$

1. Linear Theory
   (a) $\omega^2 = \omega_e^2 + 3(kv_e)^2$
   Foreshock: $v_e = \frac{dx}{DIFF}$
   (b) $\omega > \omega_e$
   (c) $\omega < \omega_e$
2. Beam Propagation
   (a) Plateau formation
   (b) Scattering into nonresonant modes
   (c) Beam injection and convection

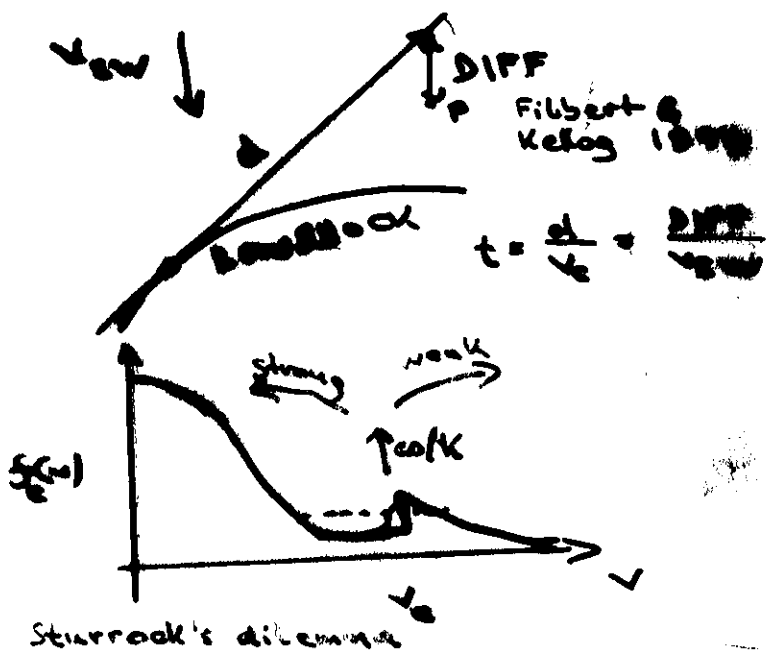

weak & strong turbulence

$\gamma_L \propto \frac{1}{v_b^2}$ <-> $\gamma_{NL} \propto \frac{N}{T_e}$

$v = \frac{x}{t}$ velocity dispersion

reabsorption of

2. Linear Instability Theory

2.1. *Fluid model* (Hybrid code)

$$\frac{dn_j}{dt} + n_j \frac{\partial}{\partial \mathbf{x}} \cdot \mathbf{u} = 0$$

$$n_j m_j \frac{d\mathbf{u}}{dt} + \frac{\partial}{\partial \mathbf{x}} \cdot P = n_j e_j (\mathbf{E} + \frac{1}{c}\mathbf{u} \times \mathbf{B}) + \frac{\delta n_j m_j \mathbf{u}}{\delta t}$$

$$\frac{d}{dt} P_{rs} + P_{rs} \frac{\partial}{\partial \mathbf{x}} \cdot \mathbf{u} + P_{rt} \frac{\partial u_s}{\partial x_t} + P_{st} \frac{\partial u_r}{\partial x_t} + \frac{\partial}{\partial x_t} Q_{trs}$$
$$= (P \times \Omega - \Omega \times P)_{rs} + \frac{\delta P_{rs}}{\delta t}$$

where $\frac{d}{dt} = \frac{\partial}{\partial t} + \mathbf{u} \cdot \frac{\partial}{\partial \mathbf{x}}$

$$\frac{n_k}{n}[1 - 3\frac{\mathbf{k} \cdot P \cdot \mathbf{k}}{nm(\omega - \mathbf{k} \cdot \mathbf{u})^2}] = \frac{1}{(\omega - \mathbf{k} \cdot \mathbf{u})^2}[i\frac{e_j}{m_j}\mathbf{k} \cdot \mathbf{E}_k + \frac{\mathbf{kkk} : Q}{n_j m_j (\omega - \mathbf{k} \cdot \mathbf{u})}]$$

$$\epsilon_j(\omega, \mathbf{k}) = -\frac{4\pi e_j n_k}{k^2 \Phi_k}$$

where $\mathbf{E}_k = -i\mathbf{k}\Phi_k$ for $e^{i(\mathbf{k}\cdot\mathbf{x} - \omega t)}$ dependence

$$\epsilon_j(\omega, \mathbf{k}) = -\frac{\omega_j^2}{(\omega - \mathbf{k} \cdot \mathbf{u})^2 - 3\mathbf{k} \cdot P \cdot \mathbf{k}/n_j m_j}$$

reflecting heat flux for $|\omega - \mathbf{k}\cdot\mathbf{u}/kv_j| \gg 1$, $B = 0$, $\omega_j^2 = \frac{4\pi n_j e_j^2}{m_j}$.

adiabatic pressure law: $p = p_0(n/n_0)^\alpha$, $\alpha = 3$.

$|\omega - \mathbf{k}\cdot\mathbf{u}/kv_j| \ll 1$: $\alpha = 1$.

Langmuir waves: $\epsilon(\omega,\mathbf{k}) = 1 + \epsilon_e = 0$: $\omega^2 = \omega_e^2 + 3(kv_e)^2$

ion sound ($T_e \gg T_i$): $\epsilon(\omega,\mathbf{k}) = 1 + \epsilon_e + \epsilon_i = 0$ $\quad \epsilon_e = \frac{1}{(k\lambda_e)^2}$

$$\omega^2 = \frac{(kc_s)^2}{1 + (k\lambda_e)^2} + 3(kv_i)^2$$

where $c_s^2 = ZT_e/M$, $\lambda_e = v_e/\omega_e$.

2.2. *Kinetic Theory*

$$\epsilon_j(\omega,\mathbf{k}) = \frac{\omega_j^2}{k^2}\int d\mathbf{v}\mathbf{k}\cdot\frac{\partial f}{\partial \mathbf{v}}\frac{1}{\omega - \mathbf{k}\cdot\mathbf{v}}$$

$$-Im\epsilon_j = \frac{\omega_j^2}{k^2}\int d\mathbf{v}\mathbf{k}\cdot\frac{\partial f}{\partial \mathbf{v}}\frac{\gamma}{(\omega - \mathbf{k}\cdot\mathbf{v}) + \gamma^2} \to \frac{\omega_j^2}{k^2}\pi\frac{\partial f}{\partial v}|_{v=\omega/k}$$

resonance width $\gamma/k \ll v_j$: kinetic **instability** (**dissipative**, resonant)

$$Re\epsilon_j = -(\frac{\omega_j}{\omega'})^2[1 + 3(\frac{kv_j}{\omega'})^2 + \ldots]$$

asymptotic expansion for $|\omega'| \gg kv_j$, $\omega' = \omega - \mathbf{k}\cdot\mathbf{u}$: **fluid model** to **lowest order**

ion sound: expansion for $|\omega'| \ll kv_e$ $\quad$ dep. on shape of $f_e(v)$

$\langle \frac{1}{v}\frac{\partial f}{\partial v}\rangle$

$Im\epsilon \neq 0$

2.3. *Reactive and Kinetic Beam Instability*

Kinetic Instability of Langmuir waves: gentle bump on tail

$$\gamma = -\frac{Im\epsilon}{\frac{\partial \epsilon}{\partial \omega}}$$ — Dissipation rate; — wave energy

$\frac{\partial f}{\partial v}\Big|_{v_\phi} > 0$

$\omega \frac{\partial \epsilon}{\partial \omega} = 2(\omega/\omega_e)^2$ $\quad \omega^2 \approx \omega_e^2 + 3v_t^2 k_e^2$

resonant particles, neglect effect of beam on real dispersion

Reactive instability:

- Fluids or $|\omega - \mathbf{k}\cdot\mathbf{u}| \gg kv_j$
- Rectangular velocity distribution (Bohm, Gross, 1949)

2 Real solutions: Bifurcation: Complex conjugate solution

independent of resonant particles phase bunching

bifurcation: $\epsilon = 0, \quad \frac{\partial \epsilon}{\partial \omega} = 0$ $\quad \delta \neq 0$!

$$\frac{k_c u}{\omega_e} = [1 + \hat{n}_b^{1/3}]^{3/2} \qquad \frac{\omega_c}{\omega_e} = [1 + \hat{n}_b^{1/3}]^{1/2}$$

$\hat{n}_b = n_b/n_e$, $\hat{T}_b = (v_b/u)^2$

$$\hat{T}_b \ll \hat{n}_b^{2/3}$$

$\hat{n}_b = 0.01$

0.0464

for reactive instability near synchronism $\omega \approx \mathbf{k}\cdot\mathbf{u}$

small k: (C. T. Dum, JGR 94, 2429-2442, 1989)

$$\hat{T}_b < \frac{1}{3}\hat{n}_b(1 - 3\hat{T}_e)$$

Fig. 1

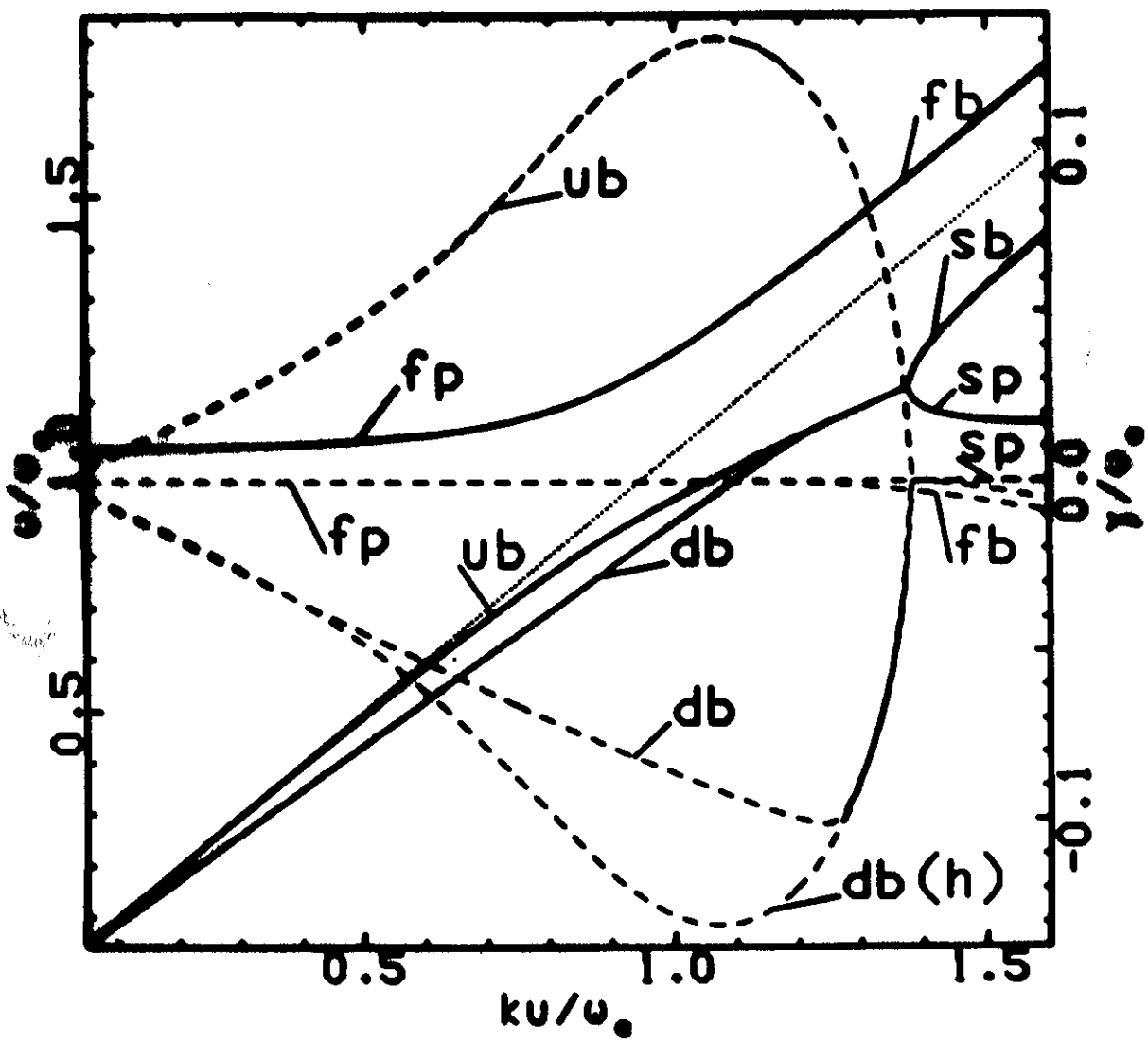

$\hat{T}_b = n_b/mu^2 < \frac{1}{3}\hat{n}_b(1-3\hat{T}_e)$ → reactive beam instab

0.001 0.01 0.01

$\hat{n}_b = \frac{n_b}{n_e} = 0.01$

b. hydrodyn. approximation

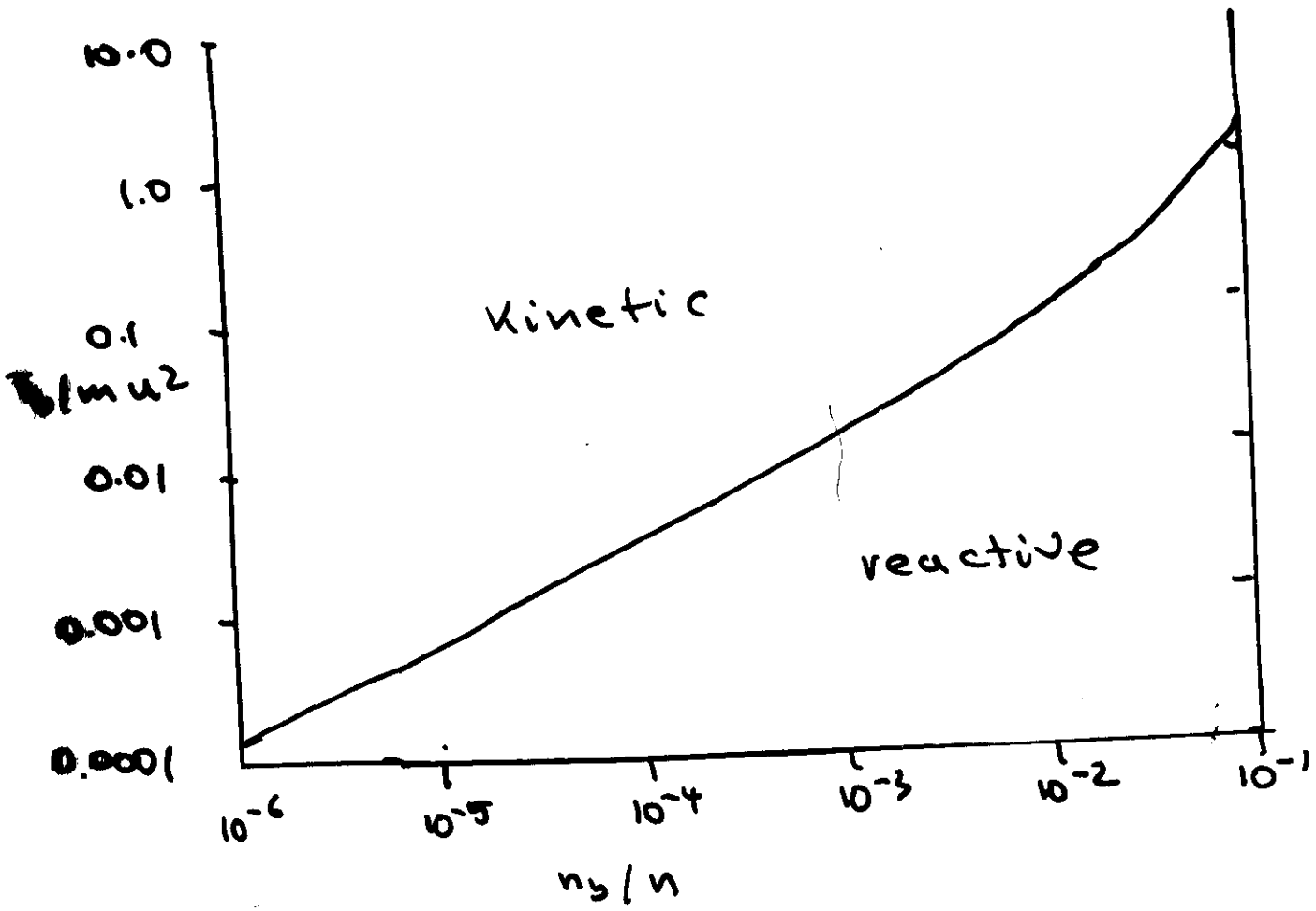

Critical beam temperature for transition to Langmuir branch (connection of fast & slow branch)

Fig. 4

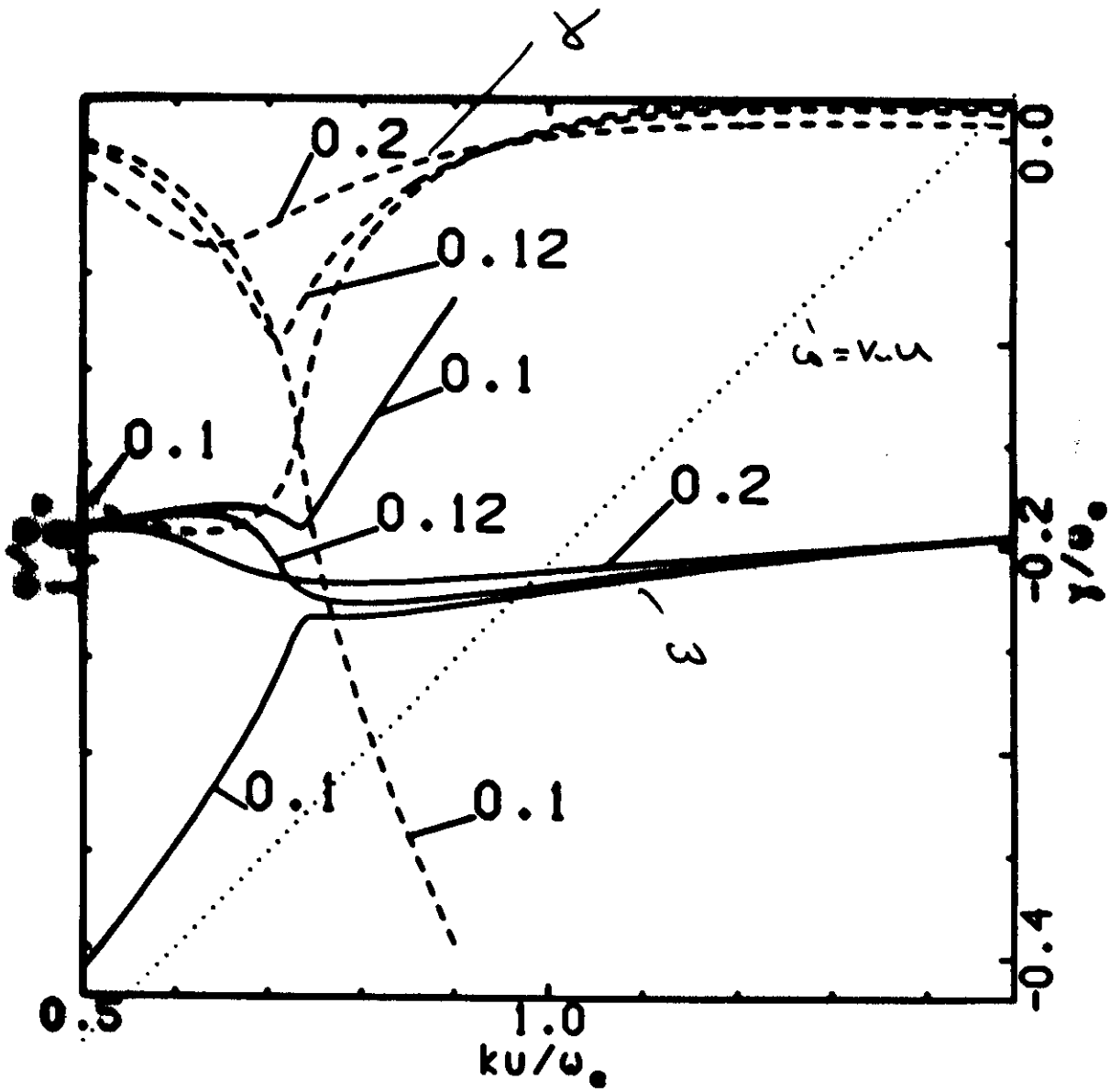

$$\hat{T}_b = \left(\frac{v_b}{v_t}\right)^2$$

$\hat{n}_b = 0.01 = \frac{n_b}{n_i}$ $\quad \hat{T}_e = 0.01 = \left(\frac{v_e}{v_t}\right)^2$

Change in topology with beam temperature: reactive/kinetic transition at $T_b = 0.105$ fast and slow plasma branch

Simulation of Gentle Bump-on-tail Instability

1) Minimum beam spread for kinetic instability of Langmuir waves:

$$\omega^2 \approx \omega_e^2 + 3k^2 v_e^2$$

2) Quasilinear and other turbulence theories require:

a. large $\Delta k \sim v_b$

many modes: periodic boundary conditions

$$k = \frac{2\pi m}{L} \qquad m = 0, 1, 2 \ldots$$

c) low fluctuation level $\frac{W}{nT_e}$

$$W \propto n_b m_b u^2/2 \qquad \gamma \approx \frac{n_b}{v_b^2}$$

$$\alpha \propto n_b m_b u v_b$$

$$W \gg W_{th}$$

3) can use hybrid model:

bulk fluid

beam particles: $\frac{dv}{dt} = \frac{e_j}{m_j} E \quad \frac{dx}{dt} = v$

for $T_e \leq 0.01 - 0.02$, $\hat{n}_b \ll 1$

DOM, 1980

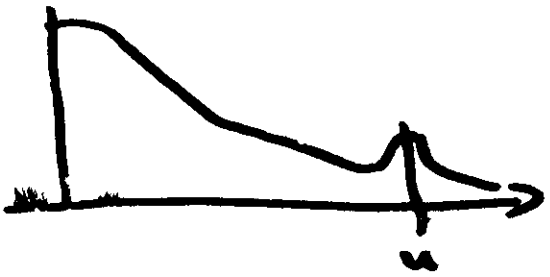

Fig. 1

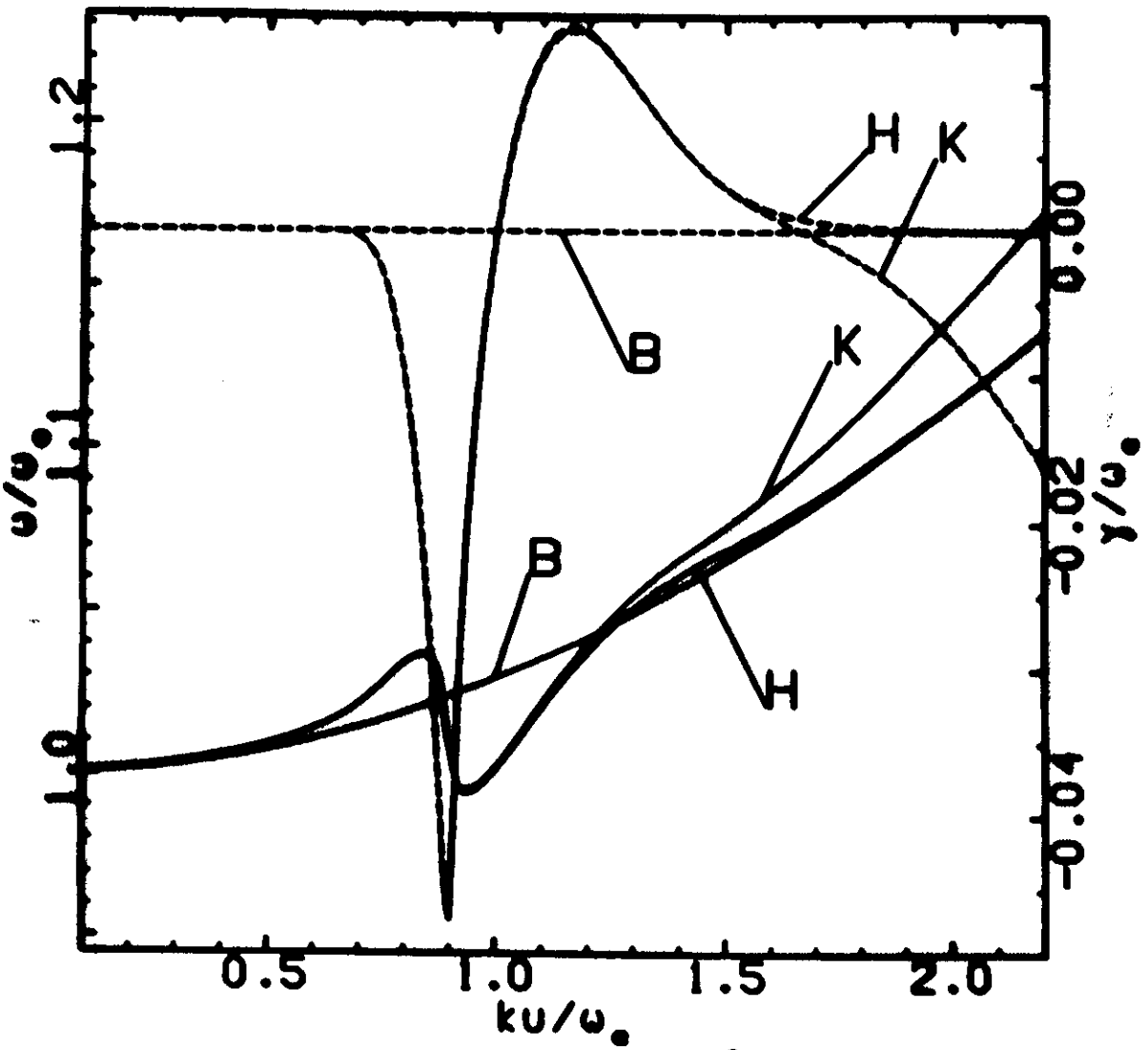

B Bohm - Gross $\omega^2 = \omega_e^2 + \frac{3}{2}(ku)^2$ $\hat{n}_b = n_b/n = 0.01$

H Hybrid (Bulk fluid) $\hat{T}_b = T_b/mu^2 = 1.65\ 10^{-2}$

K Kinetic $\hat{T}_e = T_e/mu^2 = 0.02$

$(u/v_e = 7.07)$

Hybrid Simulation
e bulk fluid
e beam particles

$\frac{n_b}{n} = 10^{-3}$

$\frac{n_b}{n m u^2} = 1.65\ 10^{-2}$

$\frac{I_e}{n m u^2} = 0.02$ ($\frac{u}{v_e} = 7.0$

Fig. 1

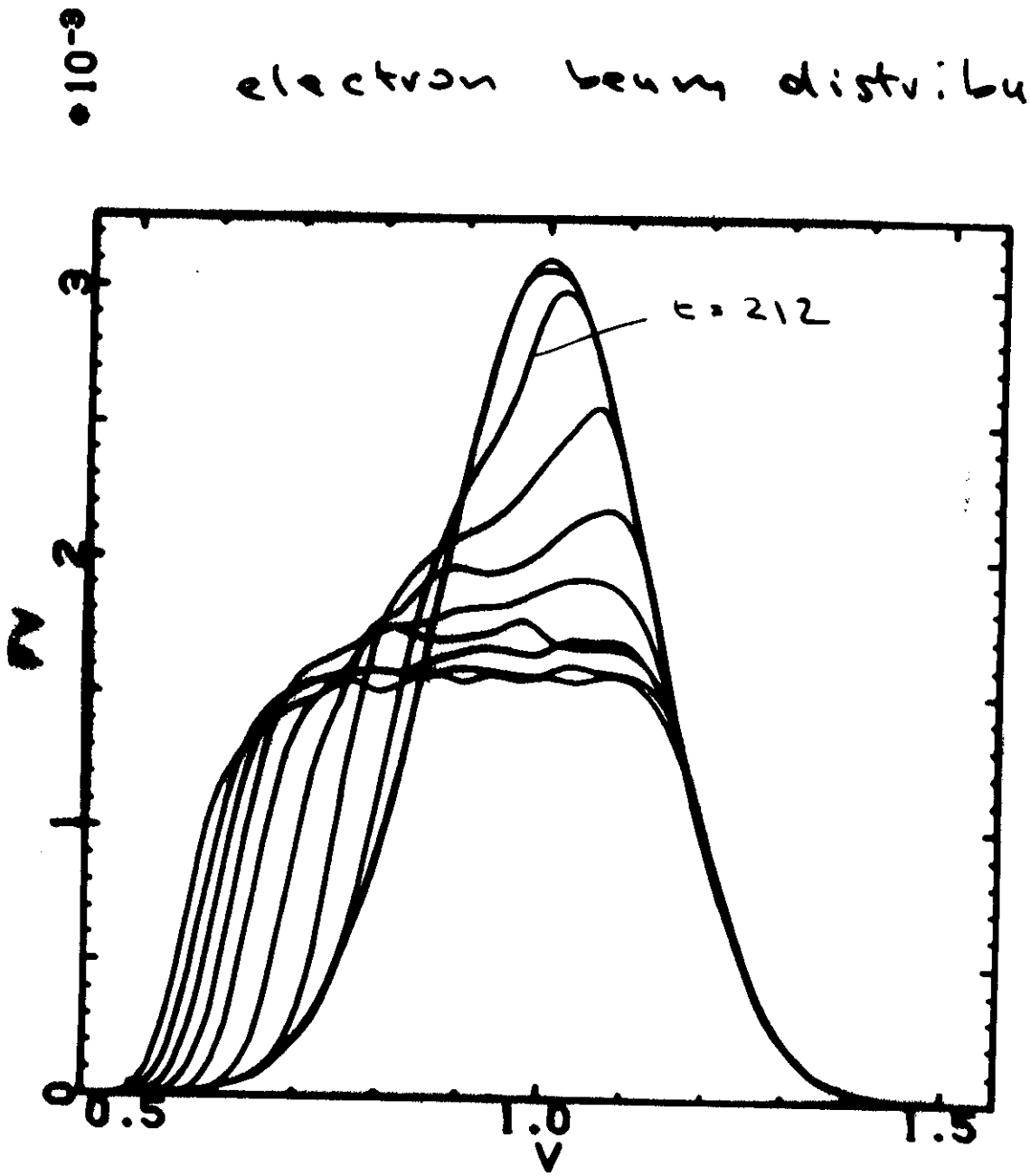

t = 4, 108, 212, 316, 420, 524, 628, 732, 836, 940 ω_{pe}^{-1}

C. T. DUM
J. G. R. 95, 80[illegible]
(1990)

C. T. DUM J. Geophys. Res 85, 8095, 1980

$W_{is} = \frac{\langle E^2 \rangle / 8\pi}{nmu^2}$

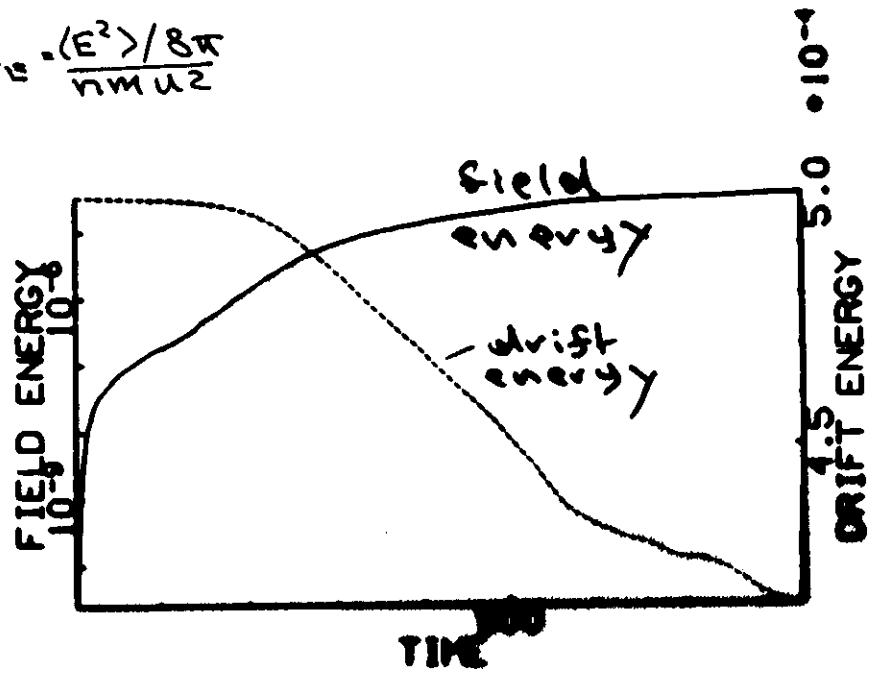

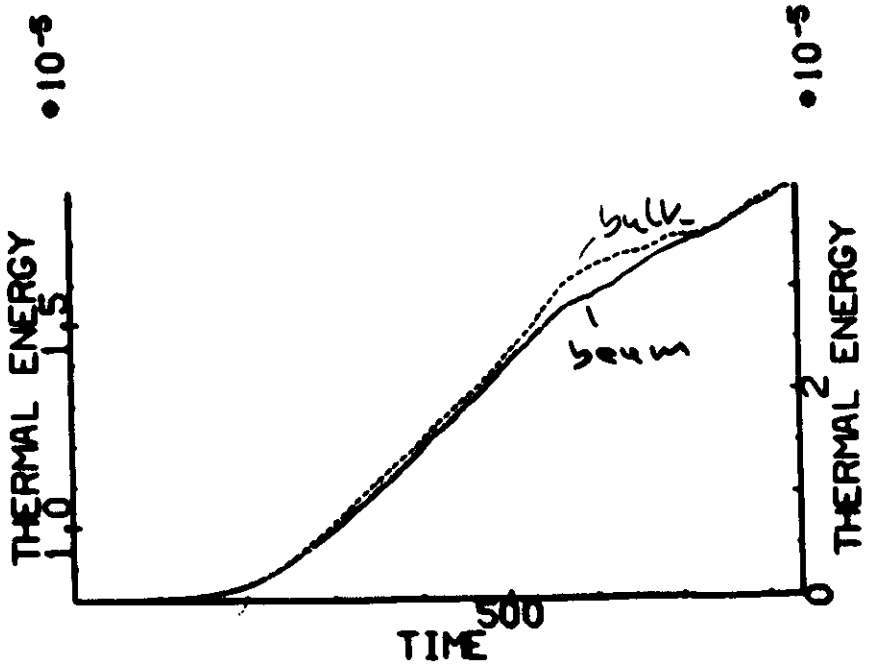

$f_b = 0.001$ $f_e = 0.02$

$f_b = 1.65\ 10^{-2}$

$k = \frac{2\pi m}{L}$ $m = 0, 1, 2..$ $L = 560\,\lambda_{DE} = 3960\,\lambda_e$

$L = N_G \Delta x$ $N_G = 2048$

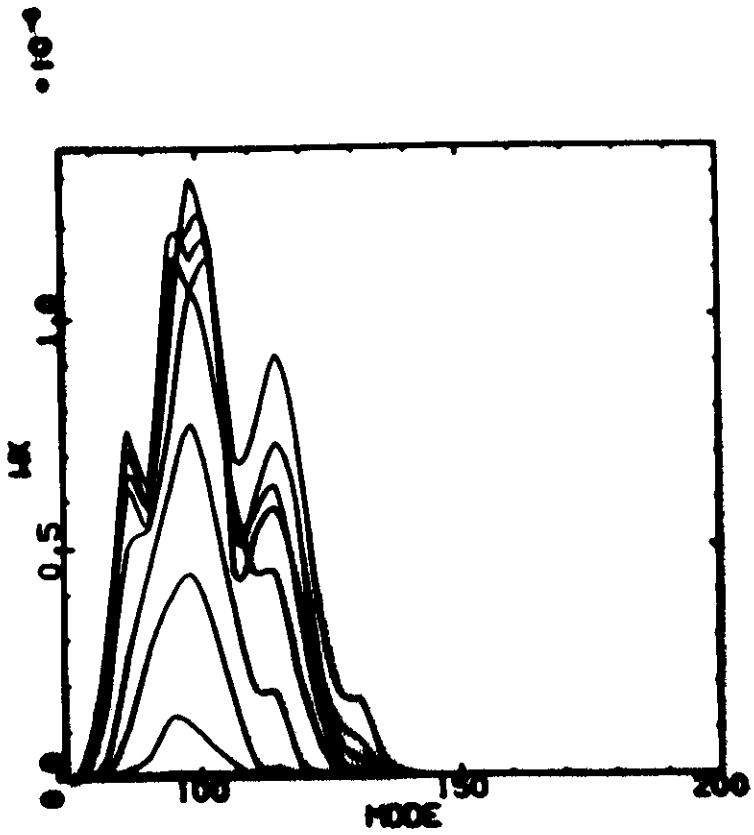

Quasilinear integral: $\Delta f \leftrightarrow W(k)$

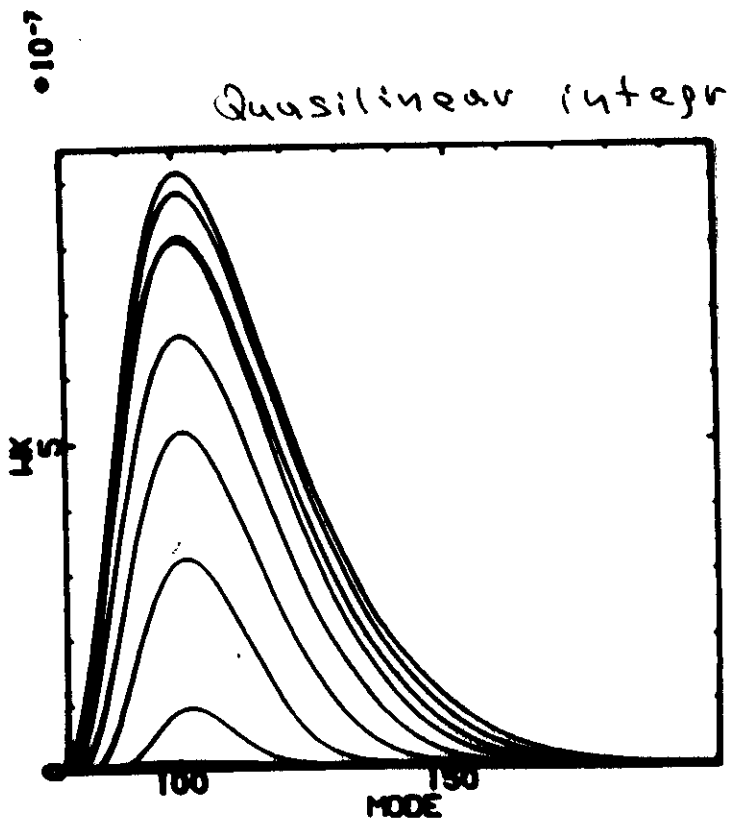

t = 4, 108, 212, 316, 420 524 628 732 836 940

Fig. 7

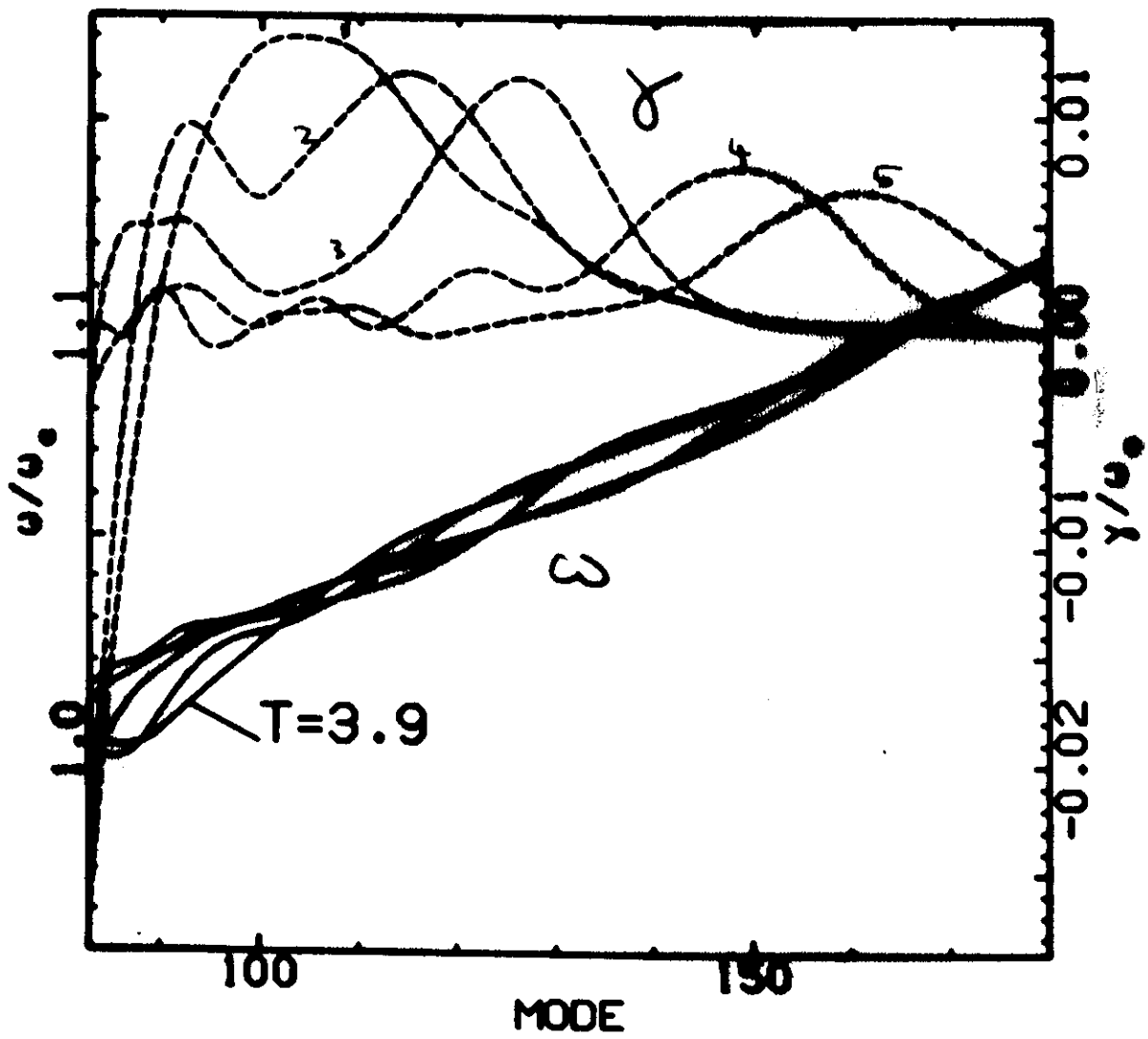

t> 3.9 , 212 , 315 , 524 , 732

Fig. 8

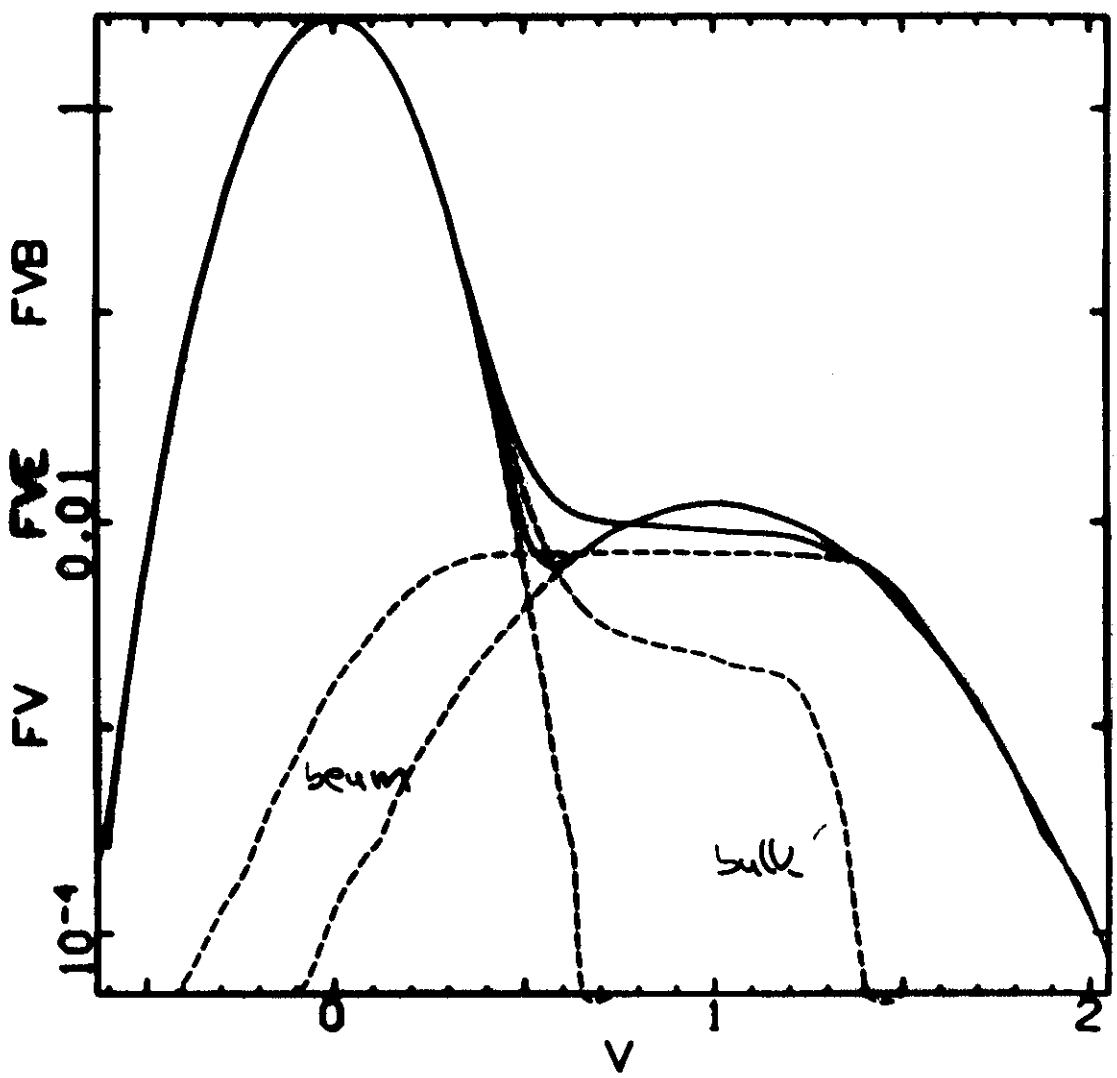

$\hat{n}_b = 0.01$ $\hat{T}_b = 0.105$ $\hat{T}_e = 0.02$

$t \omega_{pi} = 2709$

Fig. 9

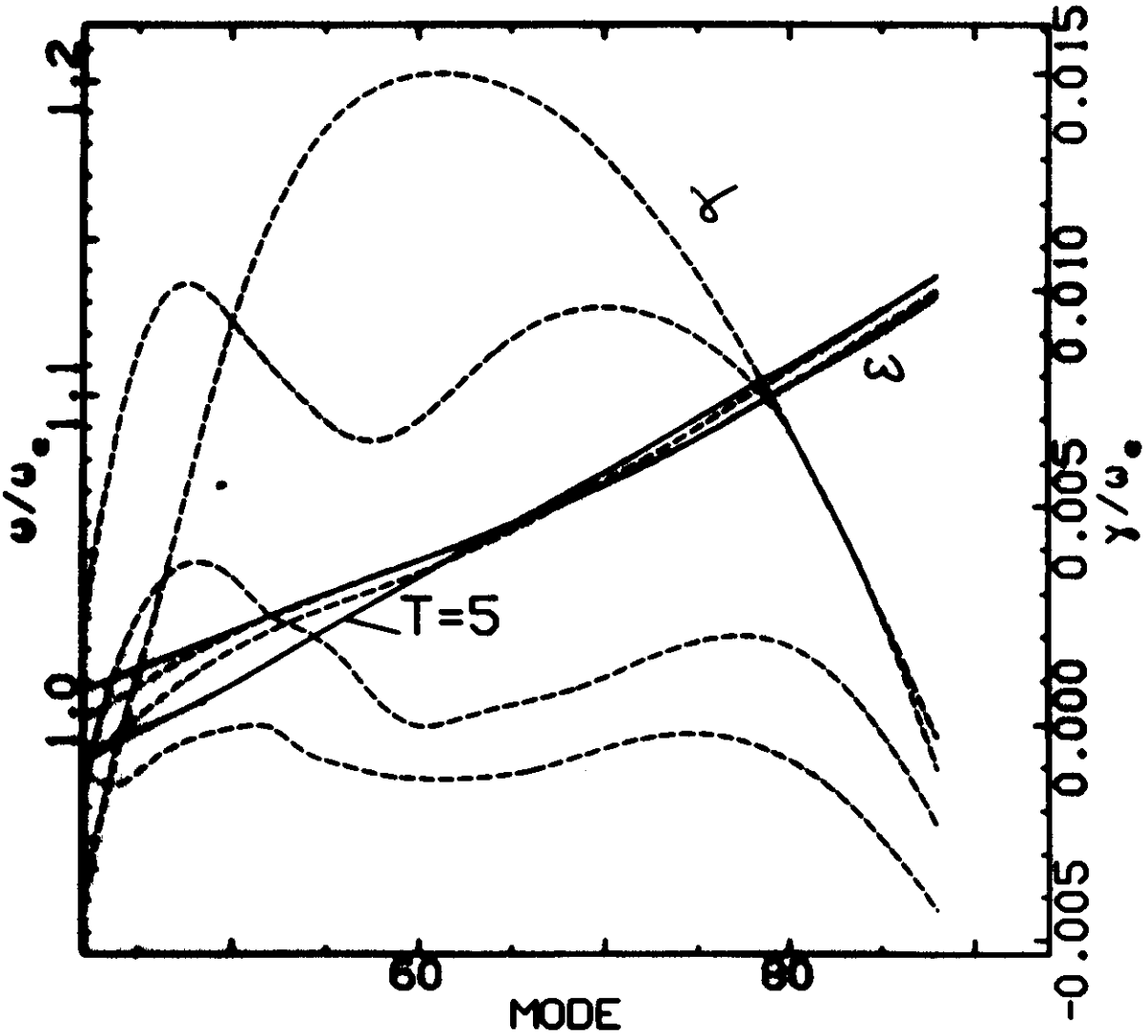

t = 5, 141, 275, 410

TIME= 681.07 YMAX=5.45E-06

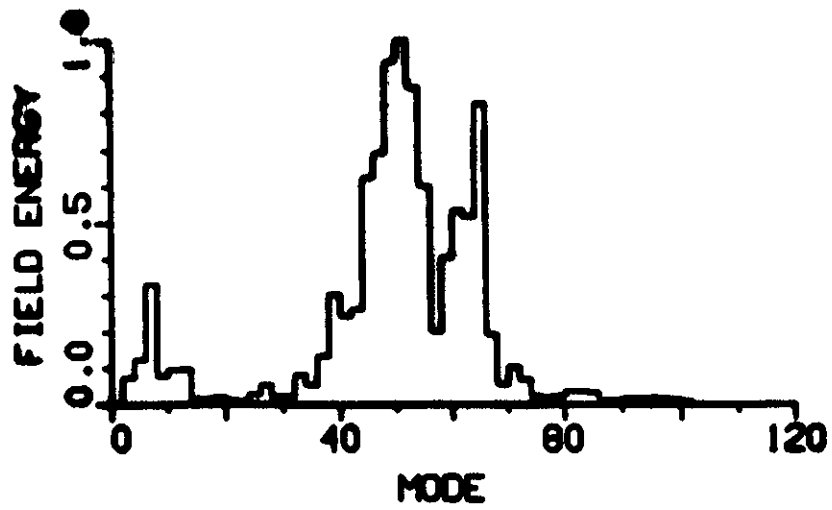

TIME= 2573.07 YMAX=1.42E-06

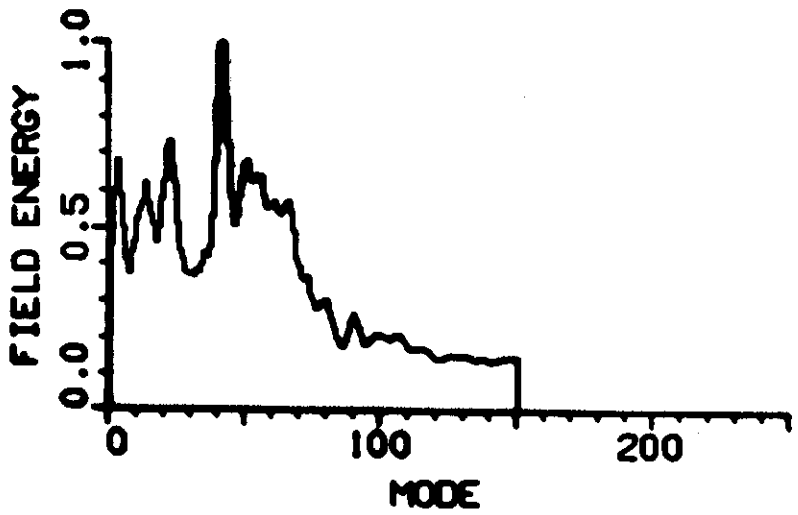

Ions included

($M/m = 100$, $T_i = T_e$)

Fig. 14

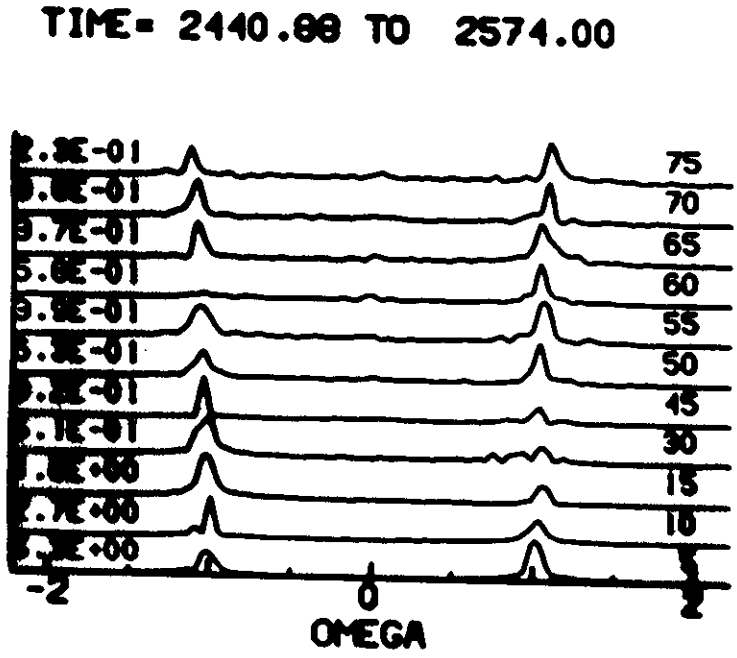

backscattered waves (eps)

Fig. 17

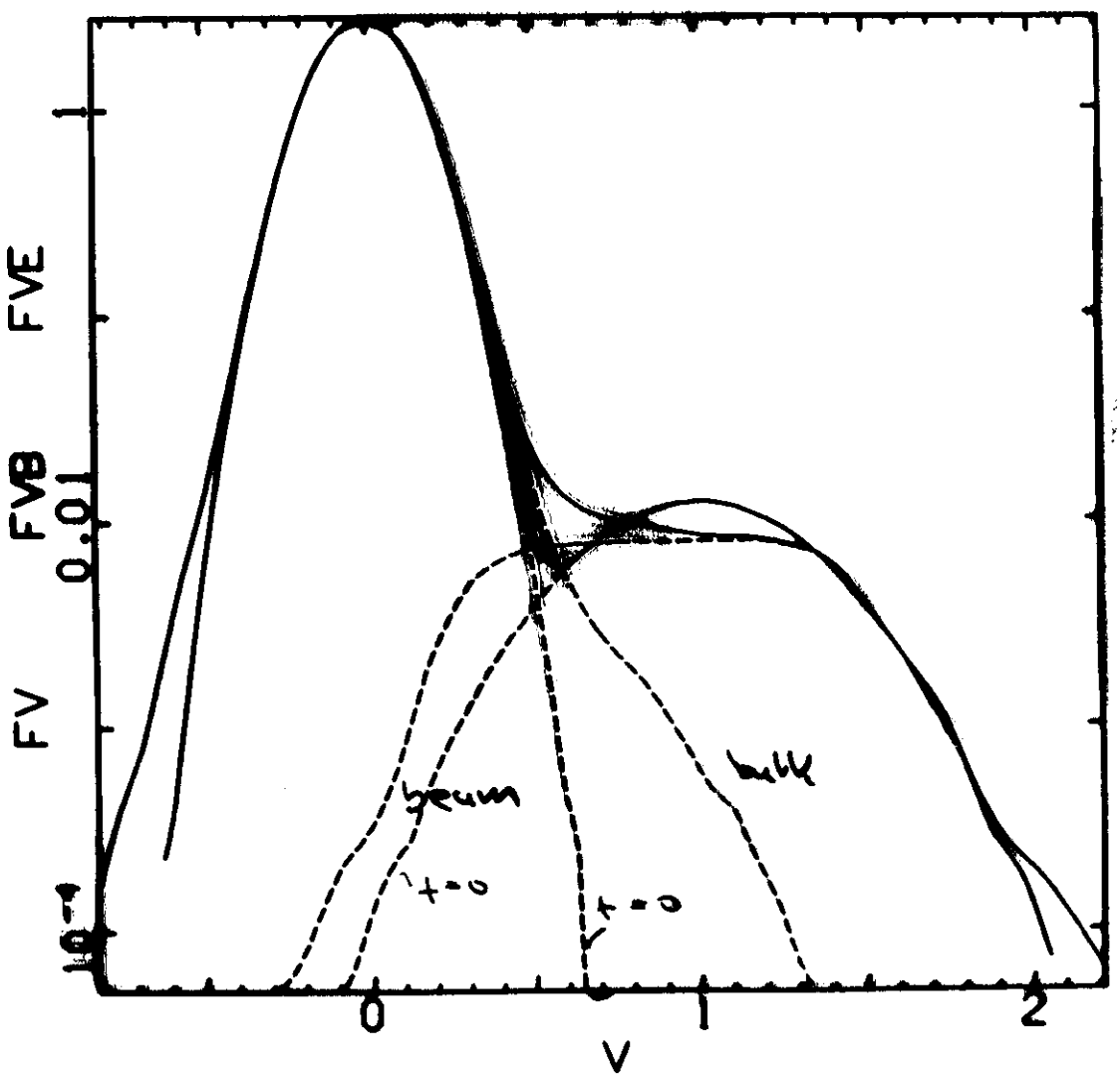

$n_b/n = 0.01$
$T_b/mu^2 = 0.105$
$T_e/mu^2 = 0.02$

$t = 5,2709$